Available online at www.sciencedirect.com

ScienceDirect

Mendeleev Commun., 2023, **33**, 679–681

Mendeleev Communications

Enhancing perovskite solar cells efficiency *via* bulk passivation of light absorbing material with L-cysteine hydrochloride

Natalia N. Udalova,[a] Nikita N. Chertorizhskiy,[a] Elizaveta N. Nemygina,[a] Artem V. Trubnikov,[b] Alexander V. Kurkin,[b] Eugene A. Goodilin[a,b] and Alexey B. Tarasov*[,a,b]

[a] *Department of Materials Science, M. V. Lomonosov Moscow State University, 119991 Moscow, Russian Federation. E-mail: alexey.bor.tarasov@yandex.ru*

[b] *Department of Chemistry, M. V. Lomonosov Moscow State University, 119991 Moscow, Russian Federation*

DOI: 10.1016/j.mencom.2023.09.028

L-Cysteine hydrochloride (CysCl) has been found to be an effective additive to hybrid halide perovskites, improving both the quality of perovskite films and the *operando* parameters of perovskite solar cells. The origin of the CysCl effect on the mixed-cation hybrid halide perovskite and related photovoltaic devices has been disclosed.

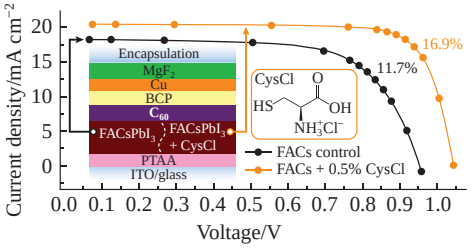

Keywords: perovskite solar cells, defect passivation, L-cysteine hydrochloride, power conversion efficiency increase, hybrid halide perovskites.

Perovskite solar cells (PSCs) based on hybrid halide perovskites are considered as a highly perspective type of photovoltaic devices with low production costs and a record power conversion efficiency (PCE) of 26%.[1] Such high PCE values were achieved by combining methods for optimizing the solar cell architecture[2,3] and perovskite composition,[4] interface engineering,[5] defect passivation,[6,7] *etc.* The latter approach is based on the use of various organic or inorganic compounds as perovskite bulk and/or surface passivators, which make it possible to noticeably reduce the defect density and improve the optoelectronic properties and microstructure of the light-harvesting material.[8,9]

Due to the ionic nature of hybrid perovskites and the corresponding defects (*e.g.*, $V_I^{\bullet}$, V_A', I_i', $Pb_{Pb}^{\delta+}$, *etc.*),[†] organic molecules with charged functional groups demonstrate better efficiency as defect passivators than neutral molecules.[10] The most perspective are positively charged ammonium groups ($–NH_3^+$, $–NMe_3^+$, *etc.*) and negatively charged $–COO^-$, I^-, Br^-, Cl^-, SO_4^{2-}, mercapto and hydroxyl groups.[9,11] The above groups could interact with the corresponding vacancies and undercoordinated atoms, as well as modulate the crystallization of perovskite from solution with an additive.[12,13] As a result, the most promising and effective passivators for hybrid halide perovskites are multifunctional organic salts (halides, sulfates, *etc.*), exerting a combined effect on the defect structure and optoelectronic properties of the light harvesting material.[14,15] In this work, we propose L-cysteine hydrochloride (CysCl) as a multifunctional additive to a perovskite solution that simultaneously contains –SH, $–NH_3^+$, Cl^- and –COOH groups. Previously, this salt was successfully used in PSCs as a modifier of interfaces between perovskite and different charge-selective layers.[16–19] In all cases, CysCl improved the interface quality and the PSCs efficiency and stability. Additionally, the L-cysteine molecule has been used as an antioxidant additive to Sn-based hybrid perovskites, preventing the oxidation of Sn^{+2} to the Sn^{+4} state.[20] In the present work, CysCl was used as a bulk additive to Pb-based mixed-cation perovskite $FA_{0.85}Cs_{0.15}PbI_3$ (FACs), where FA is the formamidinium cation $CH(NH_2)_2^+$, for a detailed analysis of its effect on perovskite properties and PSC efficiency.[‡]

According to SEM data, FACs films with 0.5 and 1% CysCl retain the initial morphology with a slight decrease in the average grain size from 177 nm for the reference to 142 and 154 nm, respectively (Figure 1). A further increase in the content of CysCl to 2.5 and 5% leads to the appearance of pinholes in FACs films and a decrease in the average grain size by 30% within a relatively wide standard deviation. Such a decrease in the grain size may

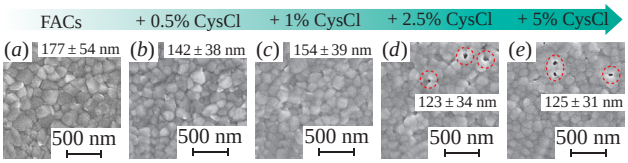

Figure 1 SEM images of FACs perovskite films obtained from solutions with the addition of (*a*) 0, (*b*) 0.5, (*c*) 1, (*d*) 2.5 and (*e*) 5% CysCl, as well as the average grain sizes of the corresponding samples.

annealing at 125 °C. Bulk passivation with CysCl was carried out by adding 0.5–5 mol% CysCl to the perovskite precursor solution. The resulting perovskite films with different CysCl content were analyzed by scanning electron microscopy (SEM), X-ray diffraction (XRD) and steady-state photoluminescence (PL) to determine the optimal CysCl concentration for use in PSCs. We also assembled a batch of PSCs and analyzed the effect of CysCl on the *operando* parameters. The experimental data obtained made it possible to reveal the impact of CysCl on the hybrid perovskite.

[†] Here, for point defects in the perovskite lattice, the Kröger–Vink notation is used, where the symbols '•' and '′' denote positive and negative effective charges, respectively, and $Pb_{Pb}^{\delta+}$ denotes surface undercoordinated lead atoms with an unknown partial positive charge.

[‡] FACs films were prepared from stoichiometric precursor solutions of formamidinium iodide, cesium iodide (CsI) and lead iodide (PbI_2) in a 4 : 1 (v/v) mixture of *N*,*N*-dimethylformamide and dimethyl sulfoxide *via* single-step antisolvent spin-coating in an inert glove box with subsequent

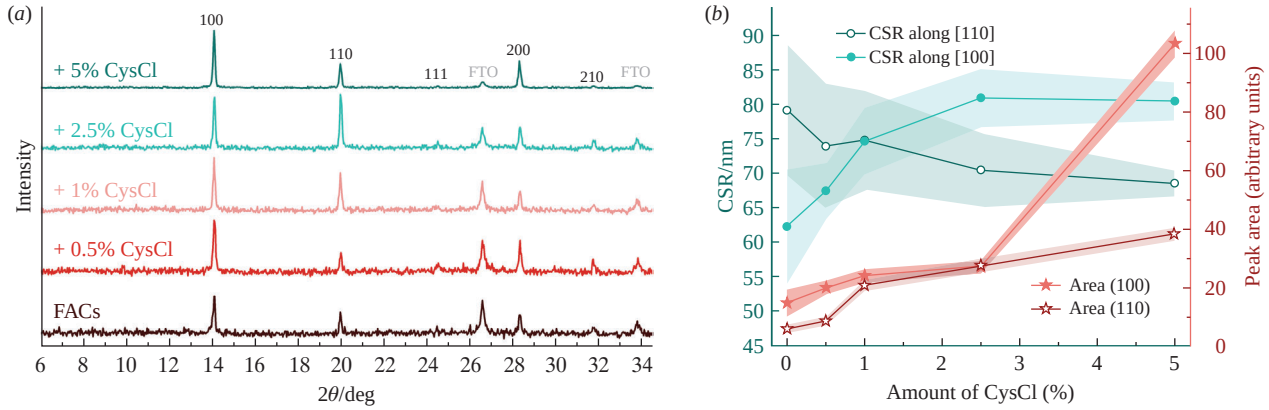

Figure 2 (*a*) XRD patterns of FACs perovskite films with different amounts of CysCl additive. (*b*) Dependences of CSR values (cyan) and peak areas (red) of (100) (●) and (110) (○) perovskite reflections, extracted from XRD patterns, on the amount of the CysCl additive.

occur due to the interaction of the –SH, –COOH and $–NH_3^+$ groups in cysteine with Pb^{2+} cations, $[PbI_x]^{2-x}$ complexes and various clusters in the perovskite solution[21,22] that could reduce the surface energy and weaken the driving force of perovskite crystallization. In the resulting modified films, cysteine cations will preferentially be localized at the grain boundaries rather than in the bulk due to the inability of large cysteine molecules to incorporate into the perovskite lattice. A similar behavior was previously observed during bulk passivation of hybrid perovskites with various salts (*e.g.*, 1,4-butanediammonium iodide[23] and *n*-hexylammonium bromide[24]).

XRD patterns of perovskite samples show the absence of any impurities, including low-dimensional perovskite-like phases with cysteine [Figure 2(*a*)]. We also performed a detailed analysis of the (100) and (110) reflections, determining their position, area, width and corresponding sizes of coherent scattering regions (CSR). Figure 2(*b*) illustrates the CSR sizes and peak areas for both (100) and (110) reflections. A consistent increase in the areas of both peaks with the addition of CysCl indicates an improvement in the crystallinity of perovskite. Interestingly, the CSR sizes demonstrate an opposite behavior between the (100) and (110) diffraction planes. With an increase in the CysCl content in perovskite films, their CSRs grow along the [100] crystallographic direction and simultaneously slightly decrease along the [110] crystallographic direction [see Figure 2(*b*)]. On the whole, it can be concluded that CysCl has a positive effect on the crystal structure of mixed-cation FACs perovskite. However, the asymmetric behavior of the CSR sizes along the [100] and [110] directions points out the appearance of a slight disorder in the perovskite intragrain domains upon the addition of CysCl, especially at higher concentrations.

Steady-state PL data demonstrate a statistically significant increase in perovskite PL intensity with the addition of CysCl [Figure 3(*a*),(*b*)]. When CysCl is added in an amount from 0 to 2.5%, the PL intensity increases linearly, and above 2.5% a plateau appears, which indicates possible saturation of the perovskite material with the additive [Figure 3(*b*)]. The statistical distribution of the full width at half maximum (FWHM) of the corresponding PL peaks, on the contrary, demonstrates a nonmonotonic dependence of this parameter on the amount of CysCl with a minimum at 0.5–1% [Figure 3(*c*)]. We hypothesize that the broadening of perovskite emission lines at ⩾2.5% CysCl could also be caused by the appearance of structural disorder, as shown in Figure 2(*b*).

According to all the above data, the optimal CysCl concentration in the bulk of perovskite appears to be 0.5–1%. These two concentrations were tested in operational perovskite solar cells and compared to control devices without CysCl added.[§]

According to *J*–*V* measurements, the CysCl additive provides a pronounced increase in PCE from ~12% for control devices to ~16.5 and ~15.5% for 0.5 and 1% CysCl, respectively [Figure 4(*a*)]. This efficiency growth is caused simultaneously by an increase in open circuit voltage (V_{OC}), short circuit current density (J_{SC}) and fill factor (FF), indicating a systematic positive effect of CysCl on perovskite microstructure, defect structure and quality of interfaces [Figure 4(*b*)–(*d*)].

Perovskite passivation also demonstrates a positive effect on the series resistance of the PSCs, decreasing R_{series} values [Figure 4(*e*)]. The shunt resistance, in turn, undergoes a pronounced 3-fold increase

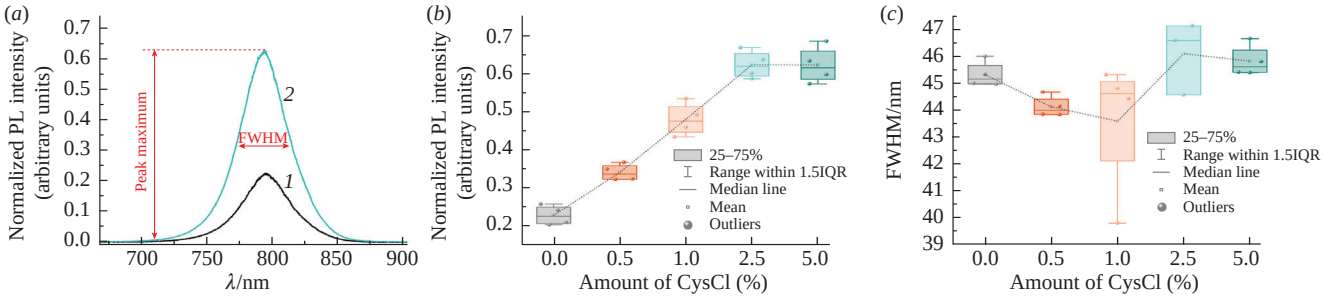

Figure 3 (*a*) Steady-state PL spectra of (*1*) FACs and (*2*) FACs + 5% CysCl perovskite films. Statistical dependence of (*b*) the intensity and (*c*) FWHM of the PL peak on the amount of CysCl.

[§] Perovskite solar cells were assembled in the inverted p–i–n architecture ITO/PTAA/perovskite/C_{60}/BCP/Cu/MgF_2. Layers of poly[bis(4-phenyl)-(2,4,6-trimethylphenyl)amine] (PTAA, 2 mg cm^{-3} in toluene), 10-carboxydecylammonium iodide (20 mM in DMF, used for better wettability of PTAA with perovskite solution) and hybrid perovskite FACs [1.5 M in DMF–DMSO (4:1, v/v)] were sequentially spin-coated onto a glass substrate with indium tin oxide (ITO) in an inert glovebox. Then, fullerene C_{60}, bathocuproine (BCP), Cu electrode and MgF_2 (a protective layer for subsequent encapsulation) were successively deposited by thermal vacuum evaporation. The resulting solar cells were eventually encapsulated with a commercially available UV-curable polymer and a cover-glass slide as described previously.[25] The *J*–*V* curves of the assembled devices were registered under simulated sunlight AM 1.5G with a power density of 100 mW cm^{-2} in a quasi-steady-state mode (20 s per point) in the reverse scanning direction.

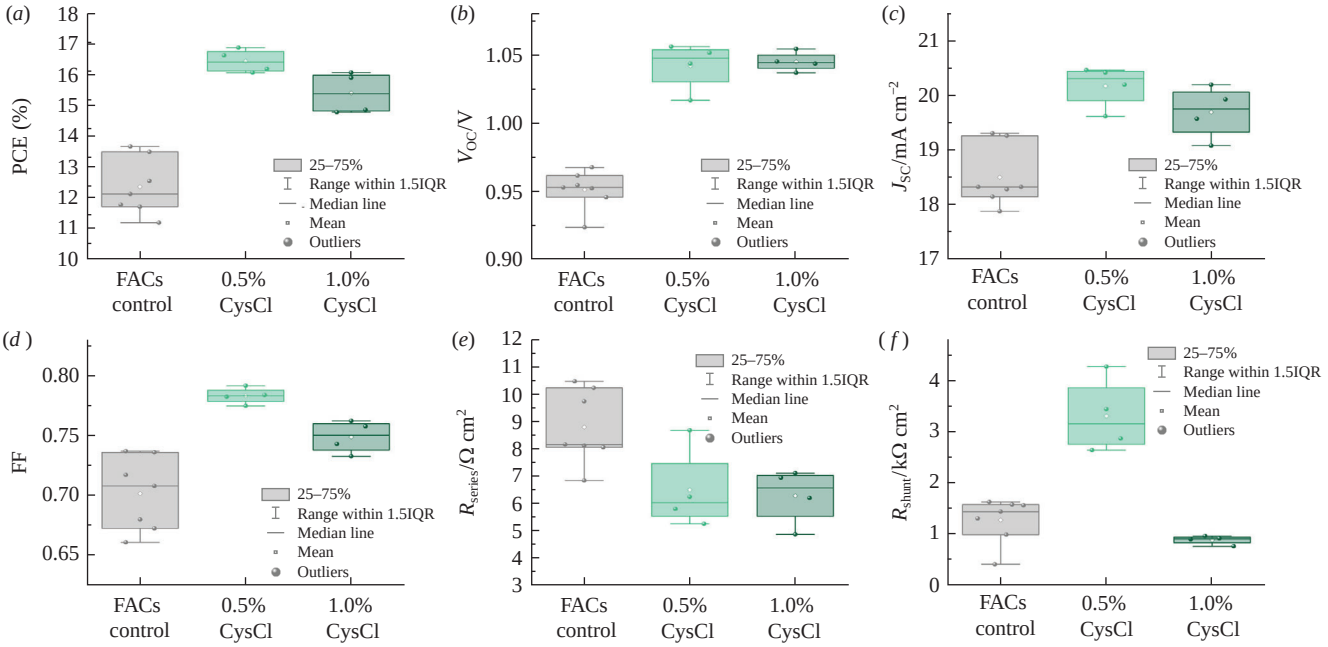

Figure 4 *Operando* parameters of PSCs based on light-harvesting materials FACs + *x*% CysCl (*x* = 0, 0.5 and 1): (*a*) PCE, (*b*) V_{OC}, (*c*) J_{SC}, (*d*) FF, (*e*) R_{series} and (*f*) R_{shunt}.

for devices with a CysCl content of 0.5%, indicating a declining number of shunts in the functional layers within the PSCs [Figure 4(*f*)]. Surprisingly, the addition of 1% CysCl does not provide an increase in the mentioned R_{shunt}, which is possibly related to the tendency for pinhole formation in perovskite films with excess CysCl content [Figure 1(*d*),(*e*)]. Most of the other *operando* PSC parameters also deteriorate for 1% CysCl, demonstrating that the optimal additive concentration would be in the region of 0.5 mol%, which is typical for similar systems (*e.g.*, in the case of bulk passivation with 1,4-butanediammonium[23]). We assume that the reason for the loss of PSC performance in the case of 1% CysCl additive is mostly based on the decrease in perovskite conductivity (J_{SC} drop) and higher parasitic resistive losses inside the devices (FF and R_{shunt} drop) compared to 0.5% CysCl additive.

In summary, L-cysteine hydrochloride was successfully used for the first time for bulk passivation of hybrid lead-iodide perovskites. This approach makes it possible to sufficiently improve both the perovskite material (higher PL intensity and better crystallinity) and the *operando* PSC parameters. It was found that the amount of CysCl 0.5% is the optimal concentration of the additive for $FA_{0.85}Cs_{0.15}PbI_3$ perovskite polycrystalline films within solar cells. In the case of 0.5% CysCl, the average value of PCE increases by 4.5%, V_{OC} by 0.1 V, J_{SC} by 2 mA cm^{-2}, FF by 0.15 and R_{shunt} by ~1500 Ω cm^2 compared to the batch of control devices.

This work was supported by the Russian Science Foundation (grant no. 22-73-00286).

References

1 NREL, *Best Research-Cell Efficiency Chart*, 2023, https://www.nrel.gov/pv/cell-efficiency.html.
2 T. Salim, S. Sun, Y. Abe, A. Krishna, A. C. Grimsdale and Y. M. Lam, *J. Mater. Chem. A*, 2015, **3**, 8943.
3 P. Roy, N. Kumar Sinha, S. Tiwari and A. Khare, *Sol. Energy*, 2020, **198**, 665.
4 H. Lu, A. Krishna, S. M. Zakeeruddin, M. Grätzel and A. Hagfeldt, *iScience*, 2020, **23**, 101359.
5 T. Wang, W. Deng, J. Cao and F. Yan, *Adv. Energy Mater.*, 2022, 2201436.
6 P. Zhao, B. J. Kim and H. S. Jung, *Mater. Today Energy*, 2018, **7**, 267.
7 Y. Li, H. Wu, W. Qi, X. Zhou, J. Li, J. Cheng, Y. Zhao, Y. Li and X. Zhang, *Nano Energy*, 2020, **77**, 105237.
8 N. Wang, Y. Zhang, P. Zeng, Y. Hu, F. Li and M. Liu, *J. Appl. Phys.*, 2020, **128**, 044504.
9 B. Chen, P. N. Rudd, S. Yang, Y. Yuan and J. Huang, *Chem. Soc. Rev.*, 2019, **48**, 3842.
10 T. Liu, P. Su, L. Liu, J. Wang, S. Feng, J. Zhang, R. Xu, H. Yang and W. Fu, *J. Mater. Chem. A*, 2019, **7**, 353.
11 S. Yang, S. Chen, E. Mosconi, Y. Fang, X. Xiao, C. Wang, Y. Zhou, Z. Yu, J. Zhao, Y. Gao, F. De Angelis and J. Huang, *Science*, 2019, **365**, 473.
12 H. T. Pham, Y. Yin, G. Andersson, K. J. Weber, T. Duong and J. Wong-Leung, *Nano Energy*, 2021, **87**, 106226.
13 X. Zheng, B. Chen, J. Dai, Y. Fang, Y. Bai, Y. Lin, H. Wei, X. C. Zeng and J. Huang, *Nat. Energy*, 2017, **2**, 17102.
14 D. Bi, X. Li, J. V. Milić, D. J. Kubicki, N. Pellet, J. Luo, T. LaGrange, P. Mettraux, L. Emsley, S. M. Zakeeruddin and M. Grätzel, *Nat. Commun.*, 2018, **9**, 4482.
15 Z. Zhang, J. Wu, S. Li, S. Liu, Q. Wang, A. Mei, Y. Rong, H. Han and Y. Hu, *Sol. RRL*, 2020, **4**, 1900248.
16 A. S. Subbiah, F. H. Isikgor, C. T. Howells, M. De Bastiani, J. Liu, E. Aydin, F. Furlan, T. G. Allen, F. Xu, S. Zhumagali, S. Hoogland, E. H. Sargent, I. McCulloch and S. De Wolf, *ACS Energy Lett.*, 2020, **5**, 3034.
17 J. He, Y. Xiang, F. Zhang, J. Lian, R. Hu, P. Zeng, J. Song and J. Qu, *Nano Energy*, 2018, **45**, 471.
18 P. Wu, X. Ma, B. Zhao, C. Liu, Y. Chen, G. Yang and X. Li, *Sustainable Energy Fuels*, 2020, **4**, 878.
19 R. Hu, W. Hou, G. Han, T. Ou, Y. Chang and Y. Xiao, *Mater. Res. Bull.*, 2022, **149**, 111698.
20 H. Mohammadian-Sarcheshmeh, M. Mazloum-Ardakani, M. Rameez, N. Mohanta and E. W.-G. Diau, *J. Nanostruct.*, 2021, **11**, 418.
21 A. S. Tutantsev, N. N. Udalova, S. A. Fateev, A. A. Petrov, C. Wang, E. G. Maksimov, E. A. Goodilin and A. B. Tarasov, *J. Phys. Chem. C*, 2020, **124**, 11117.
22 A. A. Petrov, E. I. Marchenko, S. A. Fateev, Y. Li, E. A. Goodilin and A. B. Tarasov, *Mendeleev Commun.*, 2022, **32**, 311.
23 N. N. Udalova, A. K. Moskalenko, N. A. Belich, P. A. Ivlev, A. S. Tutantsev, E. A. Goodilin and A. B. Tarasov, *Nanomaterials*, 2022, **12**, 4357.
24 S. Tang, J. Bing, J. Zheng, J. Tang, Y. Li, M. Mayyas, Y. Cho, T. W. Jones, T. C.-J. Yang, L. Yuan, M. Tebyetekerwa, H. T. Nguyen, M. P. Nielsen, N. J. Ekins-Daukes, K. Kalantar-Zadeh, G. J. Wilson, D. R. McKenzie, S. Huang and A. W. Y. Ho-Baillie, *Cell Rep. Phys. Sci.*, 2021, **2**, 100511.
25 N. A. Belich, A. A. Petrov, P. A. Ivlev, N. N. Udalova, A. A. Pustovalova, E. A. Goodilin and A. B. Tarasov, *J. Energy Chem.*, 2023, **78**, 246.

Received: 24th April 2023; Com. 23/7155